ICES REPORT 17-17

July 2017

Construction of H(div)-conforming mixed finite elements on cuboidal hexahedra

by

Todd Arbogast and Zhen Tao

The Institute for Computational Engineering and Sciences
The University of Texas at Austin
Austin, Texas 78712

Reference: Todd Arbogast and Zhen Tao, "Construction of H(div)-conforming mixed finite elements on cuboidal hexahedra," ICES REPORT 17-17, The Institute for Computational Engineering and Sciences, The University of Texas at Austin, July 2017.

CONSTRUCTION OF $H(\mathrm{div})$-CONFORMING MIXED FINITE ELEMENTS ON CUBOIDAL HEXAHEDRA*

TODD ARBOGAST† AND ZHEN TAO‡

Abstract. We generalize the two dimensional mixed finite elements of Arbogast and Correa [T. Arbogast and M. R. Correa, SIAM J. Numer. Anal., 54 (2016), pp. 3332–3356] defined on quadrilaterals to three dimensional cuboidal hexahedra. The construction is similar in that polynomials are used directly on the element and supplemented with functions defined on a reference element and mapped to the hexahedron using the Piola transform. The main contribution is providing a systematic procedure for defining supplemental functions that are divergence-free and have any prescribed polynomial normal flux. A procedure is also presented for determining which supplemental fluxes are required to define the finite element space. Both full and reduced $H(\mathrm{div})$-approximation spaces may be defined, so the scalar variable, vector variable, and vector divergence are approximated optimally. The spaces can be constructed to be of minimal local dimension, if desired.

Key words. Second order elliptic equation, mixed method, divergence approximation, full $H(\mathrm{div})$-approximation, reduced $H(\mathrm{div})$-approximation, inf-sup stable, AC spaces

AMS subject classifications. 65N30, 65N12, 41A10

1. Introduction.

It is well-known that standard mixed finite elements defined on a square or cube and mapped to a general convex quadrilateral or cuboidal hexahedron perform poorly; in fact, they fail to approximate the divergence in an optimal way or require a very high number of local degrees of freedom. Recently, Arbogast and Correa [1] resolved the problem on quadrilaterals. They defined two families of mixed finite elements that are of minimal local dimension and achieve optimal convergence properties. In this paper, we generalize these elements to convex, cuboidal hexahedra, i.e., convex polyhedra with six flat quadrilateral faces.

It is convenient to discuss $H(\mathrm{div})$-conforming mixed finite elements in the context of the simplest problem to which they apply. Let $\Omega \subset \mathbb{R}^d$, $d = 2$ or 3, be a polytopal domain, let $W = L^2(\Omega)$ and $(\cdot,\cdot)_\omega$ denote the $L^2(\omega)$ or $(L^2(\omega))^d$ inner-product, and let $\mathbf{V} = H(\mathrm{div};\Omega) = \{\mathbf{v} \in (L^2(\Omega))^2 : \nabla\cdot\mathbf{u} \in L^2(\Omega)\}$. Consider the second order elliptic boundary value problem in mixed variational form: Find $(\mathbf{u}, p) \in \mathbf{V}\times W$ such that

$$(a^{-1}\mathbf{u},\mathbf{v})_\Omega - (p,\nabla\cdot\mathbf{v})_\Omega = 0 \qquad \forall \mathbf{v}\in\mathbf{V}, \tag{1.1}$$

$$(\nabla\cdot\mathbf{u}, w)_\Omega = (f,w)_\Omega \quad \forall w \in W, \tag{1.2}$$

where $f \in L^2(\Omega)$ and the tensor a is uniformly positive definite and bounded. A mixed finite element method is given by restricting $\mathbf{V}\times W$ to inf-sup compatible finite element subspaces $\mathbf{V}_r \times W_r \subset \mathbf{V}\times W$ defined (in our case) over a mesh of convex, cuboidal hexahedra, where $r \geq 0$ is the index of the subspaces.

Full $H(\mathrm{div})$-approximation spaces of index $r \geq 0$ approximate $\mathbf{u}$, p, and $\nabla\cdot\mathbf{u}$ to order h^{r+1}, where h is the maximal diameter of the computational mesh elements. Such spaces include the classic spaces of Raviart-Thomas (RT) [13, 15] in 2-D and

*This work was supported by the U.S. National Science Foundation under grant DMS-1418752.

†Department of Mathematics, University of Texas, 2515 Speedway, Stop C1200 Austin, TX 78712-1202 and Institute for Computational Engineering and Sciences, University of Texas, 201 EAST 24th St., Stop C0200 Austin, TX 78712-1229 (arbogast@ices.utexas.edu)

‡ Institute for Computational Engineering and Sciences, University of Texas, 201 EAST 24th St., Stop C0200 Austin, TX 78712-1229 (taozhen@ices.utexas.edu)

3-D, as well as, in 2-D only, the spaces of Arnold-Boffi-Falk (ABF) [4] and Arbogast-Correa (AC) [1]. The ABF spaces have been generalized recently to 3-D by Bergot and Durufle [6]. Reduced $H(\mathrm{div})$-approximation spaces of index $r \geq 1$ approximate $\mathbf{u}$ to order h^{r+1} and p and $\nabla \cdot \mathbf{u}$ to order h^r. In this category are the classic spaces due to Brezzi-Douglas-Marini (BDM) [9] in 2-D and their 3-D counterpart from Brezzi-Douglas-Duràn-Fortin (BDDF) [7, 2], as well as the reduced Arbogast-Correa ($\mathrm{AC}^{\mathrm{red}}$) spaces [1] in 2-D. Recent progress on defining 3-D mixed finite elements has been made by many authors, including, but certainly not exhaustively, [12, 6, 2, 3, 11].

All spaces save AC, $\mathrm{AC}^{\mathrm{red}}$, and the spaces of Cockburn and Fu [11] are defined on a reference square or cube $\hat{E} = [0,1]^d$ and mapped to the element E using the Piola transform. The RT and BDM (and BDDF) spaces lose accuracy. The ABF spaces maintain accuracy, but at the expense of adding many extra degrees of freedom to the local finite element space. Cockburn and Fu construct finite elements on hexahedra using a sub mesh of tetrahedra.

The two families of AC spaces, $\mathbf{V}_r$ and $\mathbf{V}_r^{\mathrm{red}}$, are constructed using a different strategy. They use polynomials defined directly on the element and supplemented by two (one if $r = 0$) basis functions defined on a reference square and mapped via Piola. Let $\mathbb{P}_r$ denote the space of polynomials of degree up to r, and let $\tilde{\mathbb{P}}_r$ denote the space of homogeneous polynomials of exact degree r. On a convex quadrilateral element E, for which $d = 2$ and $\mathbf{x} = (x_1, x_2)$, the full $H(\mathrm{div})$-approximation spaces of index $r \geq 0$ are

$$\mathbf{V}_r(E) = (\mathbb{P}_r)^d \oplus \mathbf{x}\tilde{\mathbb{P}}_r \oplus \mathbb{S}_r(E) \quad \text{and} \quad W_r(E) = \mathbb{P}_r, \tag{1.3}$$

and the reduced $H(\mathrm{div})$-approximation spaces of index $r \geq 1$ are

$$\mathbf{V}_r(E) = (\mathbb{P}_r)^d \oplus \mathbb{S}_r(E) \quad \text{and} \quad W_r(E) = \mathbb{P}_{r-1}. \tag{1.4}$$

One can define the reference supplemental space on $\hat{E} = [0,1]^d$ in 2-D as

$$\hat{\mathbb{S}}_r = \begin{cases} \mathrm{span}\big\{\widehat{\mathrm{curl}}\big((\hat{x}_1 - 1/2)(\hat{x}_2 - 1/2)\big)\big\}, & r = 0, \\ \mathrm{span}\big\{\widehat{\mathrm{curl}}\big((\hat{x}_1 - 1/2)^{r-1}\hat{x}_1(1-\hat{x}_1)(\hat{x}_2 - 1/2)\big), & \\ \qquad \widehat{\mathrm{curl}}\big((\hat{x}_1 - 1/2)(\hat{x}_2 - 1/2)^{r-1}\hat{x}_2(1-\hat{x}_2)\big)\big\}, & r \geq 1, \end{cases} \tag{1.5}$$

and then

$$\mathbb{S}_r(E) = \mathcal{P}_E\, \hat{\mathbb{S}}_r, \tag{1.6}$$

where $\mathcal{P}_E$ is the Piola transform from $\hat{E} = [0,1]^d$ to E.

Our generalization of the two families of AC spaces has the same form (1.3)–(1.4), (1.6), with now $d = 3$ and $\mathbf{x} = (x_1, x_2, x_3)$, but the number of supplemental functions is 2 for $r = 0$ and otherwise at most $3(r+1)$. The divergences of these vectors lie in $\mathbb{P}_r$ for the full space and in $\mathbb{P}_{r-1}$ for the reduced space, and the normal flux on each edge or face f of E is in $\mathbb{P}_r(f)$ (i.e., $\mathbb{P}_r$ in dimension $d-1$). In fact, the degrees of freedom (DOFs) of a vector $\mathbf{v} \in \mathbf{V}_r$ or $\mathbf{V}_r^{\mathrm{red}}$ include the divergence and edge or face normal fluxes:

$$(\nabla \cdot \mathbf{v}, w)_E \quad \forall w \in \mathbb{P}_r^* \text{ (for } \mathbf{V}_r) \text{ or } \mathbb{P}_{r-1}^* \text{ (for } \mathbf{V}_r^{\mathrm{red}}), \tag{1.7}$$

$$(\mathbf{v} \cdot \nu, \mu)_f \quad \forall \text{ edges } (d=2) \text{ or faces } (d=3)\ f \text{ of } E \text{ and } \forall \mu \in \mathbb{P}_r(f), \tag{1.8}$$

where ν is the outer unit normal vector to E and $\mathbb{P}_r^*$ are the polynomials of degree r with no constant term. The purpose of the supplements is to make these DOFs independent, so that the elements can be joined in $H(\text{div})$ to form $\mathbf{V}_r$ or $\mathbf{V}_r^{\text{red}}$ while also maintaining consistency to approximate the divergence. The set of DOFs is completed by adding conditions on the interior, divergence-free, bubble functions (for $H(\text{div})$-conforming elements, an *interior bubble function* is a vector function with vanishing normal component on ∂E).

After setting some additional notation in Section 2, we describe how to construct arbitrary, divergence-free supplemental functions in 3-D with a prescribed normal flux in Sections 3 and 4. In Section 5, we describe a way to chose the specific supplemental functions needed to define $\mathbb{S}_r(E)$. The most useful cases $r = 0$ and $r = 1$ are given in detail. For $r \geq 1$, we need to determine the normal fluxes needed to ensure that the DOFs (1.8) are independent. We note the recent work of Cockburn and Fu [11] in this regard, but we provide a method for resolving this issue based on linear algebra. We close by presenting some numerical results in Section 6.

2. Further notation. In this section, we fix the notation and geometry used throughout the paper. As noted above, let $\mathbb{P}_r$ denote the space of polynomials of degree r. Generally, $\mathbb{P}_r = \mathbb{P}_r(\mathbb{R}^3)$ is defined over a three-dimensional domain. Sometimes we need to restrict polynomials to faces, so let $\mathbb{P}_r(f)$ be the polynomials defined over the domain f. Let $\tilde{\mathbb{P}}_r$ denote the space of homogeneous polynomials of degree r. We also let $\mathbb{P}_{r,s,t}$ denote the tensor product polynomial spaces of degree r in x_1, s in x_2, and t in x_3.

2.1. A convex, cuboidal hexahedron and the Piola map. Fix the reference element $\hat{E} = [0,1]^3$ and take any convex, cuboidal hexahedron E oriented as in Figure 2.1. The reference element $\hat{E}$ has faces ordered as follows. Face 0 is where $\hat{x}_1 = 0$ and it is denoted $\hat{f}_0 = E \cap \{\hat{x}_1 = 0\}$, face 1 is where $\hat{x}_1 = 1$ and it is denoted $\hat{f}_1$, and so forth to face 5 is where $\hat{x}_3 = 1$ and it is denoted $\hat{f}_5$. The vertices $\hat{\mathbf{x}}_{ijk}$ are indexed by the faces of intersection, i.e., $\hat{\mathbf{x}}_{ijk} = \hat{f}_i \cap \hat{f}_j \cap \hat{f}_k$. The bijective and trilinear map $\mathbf{F}_E : \hat{E} \to E$ is defined by

$$
\begin{aligned}
\mathbf{F}_E(\hat{\mathbf{x}}) &= \mathbf{x}_{024}(1-\hat{x}_1)(1-\hat{x}_2)(1-\hat{x}_3) + \mathbf{x}_{124}\,\hat{x}_1(1-\hat{x}_2)(1-\hat{x}_3) \\
&\quad + \mathbf{x}_{034}(1-\hat{x}_1)\hat{x}_2(1-\hat{x}_3) + \mathbf{x}_{134}\,\hat{x}_1\hat{x}_2(1-\hat{x}_3) \\
&\quad + \mathbf{x}_{025}(1-\hat{x}_1)(1-\hat{x}_2)\hat{x}_3 + \mathbf{x}_{125}\,\hat{x}_1(1-\hat{x}_2)\hat{x}_3 \\
&\quad + \mathbf{x}_{035}(1-\hat{x}_1)\hat{x}_2\hat{x}_3 + \mathbf{x}_{135}\,\hat{x}_1\hat{x}_2\hat{x}_3 \\
&\in \mathbb{P}_{1,1,1}.
\end{aligned} \tag{2.1}
$$

This map fixes the notation on E (faces $f_i = \mathbf{F}_E(\hat{f}_i)$ and vertices $\mathbf{x}_{ijk} = \mathbf{F}_E(\hat{\mathbf{x}}_{ijk})$). The center of face i is denoted $\mathbf{x}_i$. The outer unit normal to face i is ν_i. For example,

$$
\nu_1 = \frac{(\mathbf{x}_{134} - \mathbf{x}_{124}) \times (\mathbf{x}_{125} - \mathbf{x}_{124})}{\|(\mathbf{x}_{134} - \mathbf{x}_{124}) \times (\mathbf{x}_{125} - \mathbf{x}_{124})\|}. \tag{2.2}
$$

2.1.1. Piola transform and Jacobians. Let $D\mathbf{F}_E(\hat{\mathbf{x}})$ denote the Jacobian matrix of F_E and $J_E(\hat{\mathbf{x}}) = \det(D\mathbf{F}_E(\hat{\mathbf{x}}))$. The contravarient Piola transform $\mathcal{P}_E$ maps a vector $\hat{\mathbf{v}} : \hat{E} \to \mathbb{R}^2$ to a vector $\mathbf{v} : E \to \mathbb{R}^2$ by the formula

$$
\mathbf{v}(\mathbf{x}) = \mathcal{P}_E(\hat{\mathbf{v}})(\mathbf{x}) = \frac{1}{J_E} D\mathbf{F}_E \hat{\mathbf{v}}(\hat{\mathbf{x}}), \quad \text{where } \mathbf{x} = \mathbf{F}_E(\hat{\mathbf{x}}). \tag{2.3}
$$

For a scalar function w, we define the map $\hat{w}$ by $\hat{w}(\hat{\mathbf{x}}) = w(\mathbf{x})$, where again $\mathbf{x} = \mathbf{F}_E(\hat{\mathbf{x}})$.

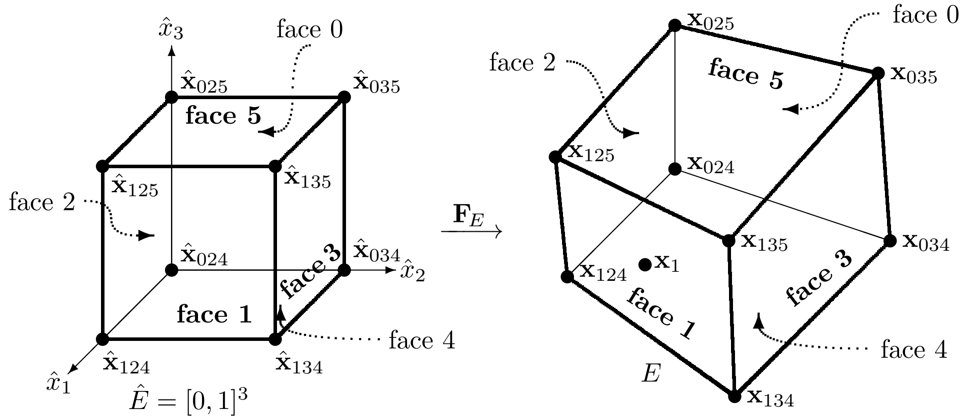

FIG. 2.1. *The geometry of the cuboidal hexahedron. On the left is the reference $\hat{E} = [0,1]^3$, which is trilinearly mapped to the hexahedron E. The faces are labeled from 0 to 5, and faces 1, 3, and 5 are in front. The corner points are labeled by their intersections with the faces (e.g., $\mathbf{x}_{135}$ intersects faces 1, 3, and 5). The centers of the faces are labeled by the face (we show only $\mathbf{x}_1$ on face 1).*

The Piola transform preserves the divergence and normal components of $\hat{\mathbf{v}}$ in the sense that

$$\nabla \cdot \mathbf{v} = \frac{1}{J_E} \hat{\nabla} \cdot \hat{\mathbf{v}}, \tag{2.4}$$

$$\mathbf{v} \cdot \nu = \frac{1}{K_i} \hat{\mathbf{v}} \cdot \hat{\nu} \quad \text{for each face } f_i \text{ of } \partial E, \tag{2.5}$$

where K_i is the face Jacobian. The face Jacobian for face i is

$$K_i = \left\| \left(\frac{\partial \mathbf{F}_E}{\partial \hat{x}_\ell} \times \frac{\partial \mathbf{F}_E}{\partial \hat{x}_m} \right)\Big|_{f_i} \right\| = \left| \left(\frac{\partial \mathbf{F}_E}{\partial \hat{x}_\ell} \times \frac{\partial \mathbf{F}_E}{\partial \hat{x}_m} \right)\Big|_{f_i} \cdot \nu_i \right|, \tag{2.6}$$

where i, ℓ, and m are distinct integers from $\{1,2,3\}$ and, say, $\ell < m$. The face Jacobian describes the bilinear distortion of the face, and it depends only on the face vertices (so two elements intersecting at face f will have the same face Jacobian). If we re-index the face so that

$$\begin{aligned} \mathbf{F}_E(\hat{x}_\ell, \hat{x}_m)\big|_{f_i} &= \mathbf{y}_0(1-\hat{x}_\ell)(1-\hat{x}_m) + \mathbf{y}_1\, \hat{x}_\ell(1-\hat{x}_m) \\ &\quad + \mathbf{y}_2(1-\hat{x}_\ell)\hat{x}_m + \mathbf{y}_3\, \hat{x}_\ell\, \hat{x}_m, \end{aligned} \tag{2.7}$$

then it is not hard to show, when f_i is flat, that

$$\begin{aligned} K_i(\hat{x}_\ell, \hat{x}_m) = {} & \|(\mathbf{y}_2 - \mathbf{y}_0) \times (\mathbf{y}_1 - \mathbf{y}_0)\|(1-\hat{x}_\ell)(1-\hat{x}_m) \\ & + \|(\mathbf{y}_3 - \mathbf{y}_1) \times (\mathbf{y}_0 - \mathbf{y}_1)\|\, \hat{x}_\ell(1-\hat{x}_m) \\ & + \|(\mathbf{y}_3 - \mathbf{y}_2) \times (\mathbf{y}_0 - \mathbf{y}_2)\|(1-\hat{x}_\ell)\hat{x}_m \\ & + \|(\mathbf{y}_2 - \mathbf{y}_3) \times (\mathbf{y}_1 - \mathbf{y}_3)\|\, \hat{x}_\ell\, \hat{x}_m \\ & \in \mathbb{P}_{1,1}. \end{aligned} \tag{2.8}$$

2.1.2. Local variables. It is clear that for the reference cube $\hat{E}$, the local variables can be taken as $\hat{x}_2$ and $\hat{x}_3$ on faces 0 and 1, $\hat{x}_1$ and $\hat{x}_3$ on faces 2 and 3, and

$\hat{x}_1$ and $\hat{x}_2$ on faces 4 and 5. Similar indexing does not necessarily hold on E. In fact, faces indexed as being opposite to each other may be far from parallel (they could even be perpendicular to each other).

It is necessary to select local variables on each face of E, two from among the set of variables $\{x_1, x_2, x_3\}$. For face ℓ, we denote these variables by (x_{i_ℓ}, x_{j_ℓ}), where we tacitly assume that $i_\ell < j_\ell$. In practice, one can find the maximal absolute component of ν_ℓ, say $|\nu_{\ell,m}|$, and omit x_m from the set $\{x_1, x_2, x_3\}$, leaving the local coordinates $\{x_{i_\ell}, x_{j_\ell}\}$.

3. Construction of Pre-supplemental Functions on the Reference Cube. In this section, we construct a vector function on the reference cube $\hat{E} = [0,1]^3$ with a vanishing divergence and prescribed monomial normal flux (up to a constant). These functions will be used later to construct the space of supplements $\mathbb{S}_r(E)$ for the new mixed finite elements. We call our special vector functions *pre-supplements.* For simplicity, we consider only face 1 (where $\hat{x}_1 = 1$). The other faces are handled analogously.

We know that vector functions exist within the BDDF spaces [7, 2] with the properties we desire. Let us fix the monomial as $\hat{x}_2^\ell \hat{x}_3^m$ for some integers $\ell \geq 0$ and $m \geq 0$. We define the pre-supplement in the more symmetric BDDF space as defined by Arnold and Awanou [2] to be, when $\ell + m \geq 1$,

$$\hat{\boldsymbol{\psi}}^1_{\ell,m} = \begin{pmatrix} \hat{x}_1 \hat{x}_2^\ell \hat{x}_3^m - \dfrac{\hat{x}_1}{(\ell+1)(m+1)} \\ \dfrac{1}{2(\ell+1)} \hat{x}_2 (1 - \hat{x}_2^\ell) \Big(\hat{x}_3^m + \dfrac{1}{m+1} \Big) \\ \dfrac{1}{2(m+1)} \hat{x}_3 (1 - \hat{x}_3^m) \Big(\hat{x}_2^\ell + \dfrac{1}{\ell+1} \Big) \end{pmatrix}. \tag{3.1}$$

We have that

$$\hat{\nabla} \cdot \hat{\boldsymbol{\psi}}^1_{\ell,m} = 0 \quad \text{and} \quad \hat{\boldsymbol{\psi}}^1_{\ell,m} \cdot \hat{\nu} = \begin{cases} \hat{x}_2^\ell \hat{x}_3^m - \dfrac{1}{(\ell+1)(m+1)} & \text{on } \hat{f}_1,\ \ell + m \geq 1, \\ 0 & \text{on } \hat{f}_i,\ i = 0, 2, \dots, 5, \end{cases} \tag{3.2}$$

where we recall that the face f_1 is where $\hat{x}_1 = 1$. The case $\ell = m = 0$ reduces to the zero vector because of the divergence theorem. We therefore accept a constant divergence and simply take

$$\hat{\boldsymbol{\psi}}^1_{0,0} = \begin{pmatrix} \hat{x}_1 \\ 0 \\ 0 \end{pmatrix}, \tag{3.3}$$

for which

$$\hat{\nabla} \cdot \hat{\boldsymbol{\psi}}^1_{0,0} = 1 \quad \text{and} \quad \hat{\boldsymbol{\psi}}^1_{0,0} \cdot \hat{\nu} = \begin{cases} 1 & \text{on } \hat{f}_1, \\ 0 & \text{on } \hat{f}_i,\ i = 0, 2, \dots, 5. \end{cases} \tag{3.4}$$

We can construct similar pre-supplements for each face; label these as $\hat{\boldsymbol{\psi}}^i_{\ell,m}$ for face $i = 0, 1, \dots, 5$.

We remark that our pre-supplemental functions are not unique when there are divergence-free bubble functions. For example, to $\hat{\boldsymbol{\psi}}^1_{\ell,m}$, one could add any function of the form

$$\begin{pmatrix} 0 \\ \dfrac{\partial}{\partial \hat{x}_3}\big[\hat{x}_2(1-\hat{x}_2)\hat{x}_3(1-\hat{x}_3)\hat{p}\big] \\ -\dfrac{\partial}{\partial \hat{x}_2}\big[\hat{x}_2(1-\hat{x}_2)\hat{x}_3(1-\hat{x}_3)\hat{p}\big] \end{pmatrix}, \tag{3.5}$$

where $\hat{p}$ is any polynomial in $\hat{x}_2$ and $\hat{x}_3$, and we would maintain (3.2).

4. Construction of the Supplemental Functions on Hexahedra. In this section, we construct a supplemental vector function $\boldsymbol{\sigma}$ with zero divergence on the convex, cuboidal hexahedron E. It has a prescribed polynomial normal flux (up to a constant) on a single face and vanishing normal flux on the other 5 faces. We continue to fix the nonzero flux on face 1 for ease of exposition; the other faces are handled similarly. In terms of the local face variables (x_{i_1}, x_{j_1}), suppose that the prescribed flux is $x_{i_1}^\ell x_{j_1}^m$. That is, we want to define $\boldsymbol{\sigma}^1_{\ell,m}$ when $\ell+m \geq 1$ so that, for some constant $c^1_{\ell,m}$,

$$\nabla\cdot\boldsymbol{\sigma}^1_{\ell,m} = 0 \quad\text{and}\quad \boldsymbol{\sigma}^1_{\ell,m}\cdot\nu = \begin{cases} x_{i_1}^\ell x_{j_1}^m - c^1_{\ell,m} & \text{on } f_1,\ \ell+m\geq 1,\\ 0 & \text{on } f_i,\ i=0,2,\ldots,5.\end{cases} \tag{4.1}$$

The construction is given by first defining an appropriate vector function $\hat{\boldsymbol{\sigma}}^1_{\ell,m}$ on the reference cube $\hat{E}$ and then mapping it to E using the Piola transform (2.3), so that $\boldsymbol{\sigma}^1_{\ell,m} = \mathcal{P}_E\hat{\boldsymbol{\sigma}}^1_{\ell,m}$. The key is to recognize that the normal components of $\hat{\boldsymbol{\sigma}}^1_{\ell,m}$ transform by (2.5), and therefore we need to include the factor K_1 within the first row of $\hat{\boldsymbol{\sigma}}^1_{\ell,m}$. Our construction is vaguely reminiscent of the one given in 2-D by Shen [14].

To proceed, we must realize two simple facts. First, the face Jacobian K_1 is bilinear in the reference variables, i.e., (2.8) holds. Second, the polynomial flux $x_{i_1}^\ell x_{j_1}^m$ is evaluated in terms of the reference variables by the map $F_E : \hat{E}\to E$ (2.1), i.e.,

$$x_{i_1} = F_{i_1}(1,\hat{x}_2,\hat{x}_3) \quad\text{and}\quad x_{j_1} = F_{j_1}(1,\hat{x}_2,\hat{x}_3), \tag{4.2}$$

which are both bilinear. Therefore the product $x_{i_1}^\ell x_{j_1}^m$, multiplied by K_1 and written in terms of the reference variables, is in the space $\mathbb{P}_{n+1,n+1}$, where $n=\ell+m$. Let the pre-image of $x_{i_1}^\ell x_{j_1}^m$ (scaled by K_1) be denoted

$$\begin{aligned} K_1 x_{i_1}^\ell x_{j_1}^m &= K_1(\hat{x}_2,\hat{x}_3)\,F_{i_1}(1,\hat{x}_2,\hat{x}_3)^\ell\,F_{j_1}(1,\hat{x}_2,\hat{x}_3)^m \\ &= \sum_{\substack{i=0\\ i+j\geq 1}}^{n+1}\sum_{j=0}^{n+1}\alpha_{ij}^{\ell,m}\Big(\hat{x}_2^i\hat{x}_3^j - \frac{1}{(i+1)(j+1)}\Big) + \alpha_{ij}^{0,0}. \end{aligned} \tag{4.3}$$

That is, in practice, we compute the coefficients $\alpha_{ij}^{\ell,m}$ based on the geometry of the hexahedron.

When $n=\ell=m=0$, let

$$\hat{\boldsymbol{\sigma}}^1_{0,0} = \sum_{i=0}^{1}\sum_{j=0}^{1}\alpha_{ij}^{0,0}\hat{\boldsymbol{\psi}}^1_{i,j}. \tag{4.4}$$

Recalling (3.2) and (3.4), this function has divergence $\alpha_{0,0}^{0,0}$ and flux K_1 on face 1. By the divergence theorem, clearly $\alpha_{0,0}^{0,0} = |f_1|$, the area of face 1, so

$$\hat{\nabla} \cdot \hat{\boldsymbol{\sigma}}_{0,0}^1 = |f_1| \quad \text{and} \quad \hat{\boldsymbol{\sigma}}_{0,0}^1 \cdot \nu = \begin{cases} K_1 & \text{on } \hat{f}_1, \\ 0 & \text{on } \hat{f}_i,\ i = 0, 2, \dots, 5. \end{cases} \tag{4.5}$$

When $n = \ell + m \geq 1$, we define

$$\hat{\boldsymbol{\sigma}}_{\ell,m}^1 = \sum_{i=0}^{n+1} \sum_{j=0}^{n+1} \alpha_{ij}^{\ell,m} \hat{\boldsymbol{\psi}}_{i,j}^1 - \frac{\alpha_{0,0}^{\ell,m}}{|f_1|} \hat{\boldsymbol{\sigma}}_{0,0}^1, \tag{4.6}$$

which has vanishing divergence and matches the flux (4.3), up to a constant multiple of K_1. Owing to (2.4)–(2.5), $\boldsymbol{\sigma}_{\ell,m}^1 = \mathcal{P}_E \hat{\boldsymbol{\sigma}}_{\ell,m}^1$ has the desired properties (4.1). We can construct a similar vector function for each face; label these as $\boldsymbol{\sigma}_{\ell,m}^i$ for face $i = 0, 1, \dots, 5$.

In the case of constant normal face fluxes (i.e., $n = 0$), we cannot remove the divergence unless we allow nonzero flux on at least two faces. We define the divergence-free supplements

$$\boldsymbol{\sigma}_{0,0}^{i,j} = \mathcal{P}_E \Big(\frac{\hat{\boldsymbol{\sigma}}_{0,0}^i}{|f_i|} - \frac{\hat{\boldsymbol{\sigma}}_{0,0}^j}{|f_j|} \Big). \tag{4.7}$$

5. Generalized AC Spaces on Convex, Cuboidal Hexahedra. We now present our generalization of the two families of AC spaces [1]. The full and reduced spaces are given by (1.3) and (1.4), respectively, once we have defined the supplemental space $\mathbb{S}_r$ for $r \geq 0$, so that the DOFs (1.7)–(1.8) are independent.

The supplemental space is constructed using the functions defined in Sections 3–4, once we know what fluxes are required to independently span the space of fluxes (1.8). To this end, it is convenient to define the flux operator $\mathcal{F}$ to be

$$\mathcal{F}(\mathbf{u}) = \big[\mathbf{u} \cdot \nu_0|_{f_o} \quad \cdots \quad \mathbf{u} \cdot \nu_5|_{f_5}\big] \subset \prod_{i=0}^{5} \mathbb{P}_r(f_i) = (\mathbb{P}_r(\mathbb{R}^2))^{1\times 6}. \tag{5.1}$$

For a sequence of n functions, we also define the "flux matrix" as

$$\mathcal{F}(\mathbf{u}_1, \dots, \mathbf{u}_n) = \begin{bmatrix} \mathcal{F}(\mathbf{u}_1) \\ \vdots \\ \mathcal{F}(\mathbf{u}_n) \end{bmatrix} = \begin{bmatrix} \mathbf{u}_1 \cdot \nu_0|_{f_o} & \dots & \mathbf{u}_1 \cdot \nu_5|_{f_5} \\ \vdots & \ddots & \vdots \\ \mathbf{u}_n \cdot \nu_0|_{f_o} & \dots & \mathbf{u}_n \cdot \nu_5|_{f_5} \end{bmatrix} \in (\mathbb{P}_r(\mathbb{R}^2))^{n\times 6}. \tag{5.2}$$

5.1. The case $r = 0$. On the convex, cuboidal hexahedron E, the new space is

$$\mathbf{V}_0(E) = \mathbb{P}_0^3 \oplus \mathbf{x}\mathbb{P}_0 \oplus \mathbb{S}_0, \tag{5.3}$$

which has only normal flux DOFs. We will give two definitions of $\mathbb{S}_0$, but first, note that $\mathbb{P}_0^3 \oplus \mathbf{x}\mathbb{P}_0$ has local dimension four, and a basis is

$$\mathcal{B}_0^{\text{poly}} = \{\mathbf{x} - \mathbf{x}_{124}, \mathbf{x} - \mathbf{x}_{034}, \mathbf{x} - \mathbf{x}_{025}, \mathbf{x} - \mathbf{x}_{024}\}. \tag{5.4}$$

The normal flux $(\mathbf{x} - \mathbf{x}_{ijk}) \cdot \nu_\ell|_{f_\ell}$ is zero if $\ell \in \{i, j, k\}$ and strictly positive otherwise.

5.1.1. A simple supplemental space. Recalling (4.7), we define simply

$$\mathbb{S}_0^{\text{simple}} = \operatorname{span}\{\boldsymbol{\sigma}_{0,0}^{1,3}, \boldsymbol{\sigma}_{0,0}^{3,5}\}. \tag{5.5}$$

A local basis is $\mathcal{B}_0^{\text{simple}} = \mathcal{B}_0^{\text{poly}} \cup \{\boldsymbol{\sigma}_{0,0}^{1,3}, \boldsymbol{\sigma}_{0,0}^{3,5}\}$. To prove that the DOFs are independent, we compute the flux matrix, which is an ordinary matrix of numbers when $r = 0$. This matrix has the sign

$$\operatorname{signum}\big(\mathcal{F}(\mathcal{B}_0^{\text{simple}})\big) = \begin{bmatrix} + & 0 & 0 & + & 0 & + \\ 0 & + & + & 0 & 0 & + \\ 0 & + & 0 & + & + & 0 \\ 0 & + & 0 & + & 0 & + \\ 0 & + & 0 & - & 0 & 0 \\ 0 & 0 & 0 & + & 0 & - \end{bmatrix}, \tag{5.6}$$

where a plus or minus sign ($+$ or $-$) indicates that the number is strictly positive or negative, respectively. Since a matrix of this form is invertible (its determinant is negative), we can decouple the DOFs (1.8); thus, the mixed finite element is well defined.

A set of shape functions can be defined by inverting $\mathcal{F}(\mathcal{B}_0^{\text{simple}})$. If we let $C = (\mathcal{F}(\mathcal{B}_0^{\text{simple}}))^{-1}$, then the shape function for the DOF on face i (i.e., $\mathcal{F}(\phi_{0,i}^{\text{simple}}) = \mathbf{e}_i^T$) is

$$\begin{aligned} \boldsymbol{\phi}_{0,i}^{\text{simple}}(x) = C_{i,1}(\mathbf{x} - \mathbf{x}_{124}) + C_{i,2}(\mathbf{x} - \mathbf{x}_{034}) + C_{i,3}(\mathbf{x} - \mathbf{x}_{025}) \\ + C_{i,4}(\mathbf{x} - \mathbf{x}_{024}) + C_{i,5}\boldsymbol{\sigma}_{0,0}^{1,3} + C_{i,6}\boldsymbol{\sigma}_{0,0}^{3,5}. \end{aligned} \tag{5.7}$$

In fact, an explicit basis can be constructed without the need to invert a matrix. Compute the positive numbers $\alpha = (\mathbf{x}_1 - \mathbf{x}_{024}) \cdot \nu_1$, $\beta = (\mathbf{x}_3 - \mathbf{x}_{024}) \cdot \nu_3$, and $\gamma = (\mathbf{x}_5 - \mathbf{x}_{024}) \cdot \nu_5$ so that

$$\mathcal{F}(\mathbf{x} - \mathbf{x}_{024}, \boldsymbol{\sigma}_{0,0}^{1,3}, \boldsymbol{\sigma}_{0,0}^{3,5}) = \begin{bmatrix} 0 & \alpha & 0 & \beta & 0 & \gamma \\ 0 & 1/|f_1| & 0 & -1/|f_3| & 0 & 0 \\ 0 & 0 & 0 & 1/|f_3| & 0 & -1/|f_5| \end{bmatrix}. \tag{5.8}$$

From these fluxes, we construct

$$\boldsymbol{\phi}_{0,1}^{\text{simple}} = |f_1| \frac{\mathbf{x} - \mathbf{x}_{024} + (|f_3|\beta + |f_5|\gamma)\boldsymbol{\sigma}_{0,0}^{1,3} + |f_5|\gamma\boldsymbol{\sigma}_{0,0}^{3,5}}{|f_1|\alpha + |f_3|\beta + |f_5|\gamma}, \tag{5.9}$$

$$\boldsymbol{\phi}_{0,3}^{\text{simple}} = |f_3| \frac{\mathbf{x} - \mathbf{x}_{024} - |f_1|\alpha\boldsymbol{\sigma}_{0,0}^{1,3} + |f_5|\gamma\boldsymbol{\sigma}_{0,0}^{3,5}}{|f_1|\alpha + |f_3|\beta + |f_5|\gamma}, \tag{5.10}$$

$$\boldsymbol{\phi}_{0,5}^{\text{simple}} = |f_5| \frac{\mathbf{x} - \mathbf{x}_{024} - |f_1|\alpha\boldsymbol{\sigma}_{0,0}^{1,3} - (|f_1|\alpha + |f_3|\beta)\boldsymbol{\sigma}_{0,0}^{3,5}}{|f_1|\alpha + |f_3|\beta + |f_5|\gamma}. \tag{5.11}$$

From these, we then construct

$$\boldsymbol{\phi}_{0,0}^{\text{simple}} = \frac{\nu_2 \times \nu_4 - (\nu_2 \times \nu_4) \cdot (\nu_1 \boldsymbol{\phi}_{0,1}^{\text{simple}} + \nu_3 \boldsymbol{\phi}_{0,3}^{\text{simple}} + \nu_5 \boldsymbol{\phi}_{0,5}^{\text{simple}})}{(\nu_2 \times \nu_4) \cdot \nu_0}, \tag{5.12}$$

$$\boldsymbol{\phi}_{0,2}^{\text{simple}} = \frac{\nu_0 \times \nu_4 - (\nu_0 \times \nu_4) \cdot (\nu_1 \boldsymbol{\phi}_{0,1}^{\text{simple}} + \nu_3 \boldsymbol{\phi}_{0,3}^{\text{simple}} + \nu_5 \boldsymbol{\phi}_{0,5}^{\text{simple}})}{(\nu_0 \times \nu_4) \cdot \nu_2}, \tag{5.13}$$

$$\boldsymbol{\phi}_{0,4}^{\text{simple}} = \frac{\nu_0 \times \nu_2 - (\nu_0 \times \nu_2) \cdot (\nu_1 \boldsymbol{\phi}_{0,1}^{\text{simple}} + \nu_3 \boldsymbol{\phi}_{0,3}^{\text{simple}} + \nu_5 \boldsymbol{\phi}_{0,5}^{\text{simple}})}{(\nu_0 \times \nu_2) \cdot \nu_4}. \tag{5.14}$$

5.1.2. A more general supplemental space. While $\mathcal{B}_0^{\text{simple}}$ is well defined and simple to implement, it is defined in a highly non-symmetric way. One could average over all similar constructions, but it is not clear how to weight them. An alternative is to add supplements that are as different as possible from the polynomial part $\mathbb{P}_0^3 \oplus \mathbf{x}\mathbb{P}_0$, and subject to the divergence-free constraint. A criterion is to consider the fluxes generated by this part, and take supplements with fluxes that span the orthogonal complement. We denote the flux matrix for $\mathcal{B}_0^{\text{poly}}$ as

$$M = \mathcal{F}(\mathcal{B}_0^{\text{poly}}) = \begin{bmatrix} a_1 & 0 & 0 & b_1 & 0 & c_1 \\ 0 & a_2 & b_2 & 0 & 0 & c_2 \\ 0 & a_3 & 0 & b_3 & c_3 & 0 \\ 0 & \alpha & 0 & \beta & 0 & \gamma \end{bmatrix}, \tag{5.15}$$

where each letter (a_i, b_i, c_i, α, β, and γ) stands for a specific positive number. The orthogonal complement of the row space of M is easily seen to be spanned by N^T, where

$$N = \begin{bmatrix} \alpha b_1/a_1 & \beta & -\beta a_2/b_2 & -\alpha & (\alpha b_3 - \beta a_3)/c_3 & 0 \\ (\beta c_1 - \gamma b_1)/a_1 & 0 & \beta c_2/b_2 & \gamma & -\gamma b_3/c_3 & -\beta \end{bmatrix}. \tag{5.16}$$

Let S denote the 6×2 matrix with rows being the desired supplemental fluxes. The divergence-free constraint can be written as $S\boldsymbol{\varphi} = 0$ in terms of the vector of face areas, which is

$$\boldsymbol{\varphi} = \big(|f_0|, |f_1|, |f_2|, |f_3|, |f_4|, |f_5|\big). \tag{5.17}$$

We define S to be the projection of N to the orthogonal complement of $\text{span}\{\boldsymbol{\varphi}\}$, i.e.,

$$S = N\Big(I - \frac{\boldsymbol{\varphi}\boldsymbol{\varphi}^T}{\boldsymbol{\varphi}^T\boldsymbol{\varphi}}\Big), \tag{5.18}$$

and then we define $\mathbb{S}_0 = \text{span}\{\boldsymbol{\sigma}_{0,0}^1, \boldsymbol{\sigma}_{0,0}^2\}$, where

$$\boldsymbol{\sigma}_{0,0}^1 = \mathcal{P}_E\big(S_{1,1}\hat{\boldsymbol{\sigma}}_{0,0}^0 + S_{1,2}\hat{\boldsymbol{\sigma}}_{0,0}^1 + S_{1,3}\hat{\boldsymbol{\sigma}}_{0,0}^2 + S_{1,4}\hat{\boldsymbol{\sigma}}_{0,0}^3 + S_{1,5}\hat{\boldsymbol{\sigma}}_{0,0}^4 + S_{1,6}\hat{\boldsymbol{\sigma}}_{0,0}^5\big), \tag{5.19}$$

$$\boldsymbol{\sigma}_{0,0}^2 = \mathcal{P}_E\big(S_{2,1}\hat{\boldsymbol{\sigma}}_{0,0}^0 + S_{2,2}\hat{\boldsymbol{\sigma}}_{0,0}^1 + S_{2,3}\hat{\boldsymbol{\sigma}}_{0,0}^2 + S_{2,4}\hat{\boldsymbol{\sigma}}_{0,0}^3 + S_{2,5}\hat{\boldsymbol{\sigma}}_{0,0}^4 + S_{2,6}\hat{\boldsymbol{\sigma}}_{0,0}^5\big), \tag{5.20}$$

since, by (4.5) and (2.4)–(2.5), these supplements satisfy the constraint of being divergence-free and produce the desired fluxes S on each face.

It remains to verify that the DOFs are independent after applying the projection. To this end, we note that $\boldsymbol{\varphi}$ is not in the span of the rows of N. This is true since $M\boldsymbol{\varphi} \neq 0$ (at least one row of M represents a function with a nonzero divergence), which implies that $\boldsymbol{\varphi} \notin (M^T)^\perp = \text{row}(N)$. Independence of the DOFs is a consequence of the following, more general lemma.

LEMMA 5.1. *Suppose that M is $m \times (m+n)$, N is $n \times (m+n)$, and $\begin{bmatrix} M \\ N \end{bmatrix}$ is invertible. Let $\boldsymbol{\varphi}$ be an $(m+n)$-vector that does not lie in the row space of N. Let the projection $P_{\boldsymbol{\varphi}} = \dfrac{\boldsymbol{\varphi}\boldsymbol{\varphi}^T}{\boldsymbol{\varphi}^T\boldsymbol{\varphi}}$. If $S = N(I - P_{\boldsymbol{\varphi}})$, then $\begin{bmatrix} M \\ S \end{bmatrix}$ is invertible.*

Proof. By a change of basis, we may assume that $M = \begin{bmatrix} I_m & 0 \end{bmatrix}$ and $N = \begin{bmatrix} 0 & I_n \end{bmatrix}$. Normalize and partition $\boldsymbol{\varphi} = \begin{pmatrix} \mathbf{a} \\ \mathbf{b} \end{pmatrix}$ into m- and n-subvectors. Now the projection in block form is

$$P_{\boldsymbol{\varphi}} = \begin{bmatrix} \mathbf{a}\mathbf{a}^T & \mathbf{a}\mathbf{b}^T \\ \mathbf{b}\mathbf{a}^T & \mathbf{b}\mathbf{b}^T \end{bmatrix},$$

and $S = \begin{bmatrix} -\mathbf{b}\mathbf{a}^T & I_n - \mathbf{b}\mathbf{b}^T \end{bmatrix}$. Since $\|\mathbf{b}\mathbf{b}^T\| < 1$ (recall $\mathbf{a} \neq 0$), we conclude that $I_n - \mathbf{b}\mathbf{b}^T$ is invertible, and thus also $\begin{bmatrix} I_m & 0 \\ -\mathbf{b}\mathbf{a}^T & I_n - \mathbf{b}\mathbf{b}^T \end{bmatrix} = \begin{bmatrix} M \\ S \end{bmatrix}$. ☐

5.2. The case $r = 1$. We concentrate on the reduced space $\mathbf{V}_1^{\text{red}}(E) = \mathbb{P}_1^3 \oplus \mathbb{S}_1$, since we merely add $\mathbf{x}\tilde{\mathbb{P}}_1$ to define $\mathbf{V}_1(E)$. The divergence of $\mathbf{V}_1^{\text{red}}(E)$ is constant as in the case $r = 0$, but now the normal face fluxes are linear, so there are 18 of them in total. Since $\dim \mathbb{P}_1^3 = 12$, we need 6 supplements.

Please recall the notation from Fig. 2.1. We can view the hexahedron as containing a tetrahedron nestled in the corner near $\mathbf{x}_{024}$, i.e., the tetrahedron with the four vertices $\mathbf{x}_{024}$, $\mathbf{x}_{124}$, $\mathbf{x}_{034}$, and $\mathbf{x}_{025}$. The usual BDM (i.e., BDDF) space on tetrahedra [7] is $\mathbb{P}_1$, so we know that we can set the fluxes independently on the faces 0, 2, and 4. Define the six linear functions

$$\lambda_i(\mathbf{x}) = -(\mathbf{x} - \mathbf{x}_i) \cdot \nu_i, \quad i = 0, 1, \dots, 5, \tag{5.21}$$

and the linear function associated with the plane f_6 through $\mathbf{x}_{124}$, $\mathbf{x}_{034}$, and $\mathbf{x}_{025}$,

$$\lambda_6(\mathbf{x}) = -(\mathbf{x} - \mathbf{x}_6) \cdot \nu_6, \tag{5.22}$$

where $\mathbf{x}_6$ lies on f_6 and ν_6 is the unit normal pointing *into* the tetrahedron.

Since $\nabla\lambda_i = -\nu_i$, we have that

$$\nabla \times (\lambda_i \lambda_j \nu_k) = -\lambda_i \nu_j \times \nu_k - \lambda_j \nu_i \times \nu_k,$$

which has no normal flux on faces i, j, and k. We claim that we can independently set the 9 fluxes on the faces 0, 2, and 4, respectively, by the functions

$$\boldsymbol{\psi}_0 = \mathbf{x} - \mathbf{x}_{124}, \quad \boldsymbol{\psi}_1 = \nabla \times (\lambda_2\lambda_6\nu_4), \quad \boldsymbol{\psi}_2 = \nabla \times (\lambda_4\lambda_6\nu_2), \tag{5.23}$$

$$\boldsymbol{\psi}_3 = \mathbf{x} - \mathbf{x}_{034}, \quad \boldsymbol{\psi}_4 = \nabla \times (\lambda_0\lambda_6\nu_4), \quad \boldsymbol{\psi}_5 = \nabla \times (\lambda_4\lambda_6\nu_0), \tag{5.24}$$

$$\boldsymbol{\psi}_6 = \mathbf{x} - \mathbf{x}_{025}, \quad \boldsymbol{\psi}_7 = \nabla \times (\lambda_0\lambda_6\nu_2), \quad \boldsymbol{\psi}_8 = \nabla \times (\lambda_2\lambda_6\nu_0). \tag{5.25}$$

The rest of the polynomial space is associated to f_6, and consists of the functions

$$\boldsymbol{\psi}_9 = \mathbf{x} - \mathbf{x}_{024}, \quad \boldsymbol{\psi}_{10} = \nabla \times (\lambda_0\lambda_2\nu_4), \quad \boldsymbol{\psi}_{11} = \nabla \times (\lambda_2\lambda_4\nu_0). \tag{5.26}$$

It is convenient for the discussion to map E to a simpler shape $\tilde{E}$ using an affine map. In the case of an affine map, no polynomial spaces are changed, so conclusions about fluxes on $\partial\tilde{E}$ hold for ∂E. We take $\tilde{E}$ as in Fig. 2.1, but it is the result of a translation that makes $\mathbf{x}_{024} = 0$. Rotations, dilations, and shear maps can then make $\mathbf{x}_{124} = \mathbf{e}_1$, $\mathbf{x}_{034} = \mathbf{e}_2$, and $\mathbf{x}_{025} = \mathbf{e}_3$. We proceed as if $E = \tilde{E}$. Then

$$\nu_0 = -\mathbf{e}_1, \quad \nu_2 = -\mathbf{e}_2, \quad \nu_4 = -\mathbf{e}_3, \quad \nu_6 = -(\mathbf{e}_1 + \mathbf{e}_2 + \mathbf{e}_3)/\sqrt{3},$$
$$\lambda_0 = x_1, \quad \lambda_2 = x_2, \quad \lambda_4 = x_3, \quad \lambda_6 = (x_1 + x_2 + x_3 - 1)/\sqrt{3}.$$

Thus, for face 0,

$$\boldsymbol{\psi}_0 = \begin{pmatrix} x_1 - 1 \\ x_2 \\ x_3 \end{pmatrix}, \quad \boldsymbol{\psi}_1 = \frac{1}{\sqrt{3}} \begin{pmatrix} 1 - x_1 - 2x_2 - x_3 \\ x_2 \\ 0 \end{pmatrix}, \quad \boldsymbol{\psi}_2 = \frac{1}{\sqrt{3}} \begin{pmatrix} x_1 + x_2 + 2x_3 - 1 \\ 0 \\ -x_3 \end{pmatrix}, \tag{5.27}$$

and so we compute the columns of $\mathcal{F}$ for faces 0, 2, and 4 as

$$\mathcal{F}(\boldsymbol{\psi}_0, \boldsymbol{\psi}_1, \boldsymbol{\psi}_2) = \begin{bmatrix} 1 & — & 0 & — & 0 & — \\ 2x_2 + x_3 - 1 & — & 0 & — & 0 & — \\ 1 - x_2 - 2x_3 & — & 0 & — & 0 & — \end{bmatrix}. \tag{5.28}$$

The other two triples, $(\boldsymbol{\psi}_3, \boldsymbol{\psi}_4, \boldsymbol{\psi}_5)$ for face 2 and $(\boldsymbol{\psi}_6, \boldsymbol{\psi}_7, \boldsymbol{\psi}_8)$ for face 4, are similar, so we conclude that indeed these 9 functions independently set the 9 fluxes on the faces 0, 2, and 4.

For the other three faces 1, 3, and 5, we have that

$$\boldsymbol{\psi}_9 = \begin{pmatrix} x_1 \\ x_2 \\ x_3 \end{pmatrix}, \quad \boldsymbol{\psi}_{10} = \begin{pmatrix} -x_1 \\ x_2 \\ 0 \end{pmatrix}, \quad \boldsymbol{\psi}_{11} = \begin{pmatrix} 0 \\ -x_2 \\ x_3 \end{pmatrix}. \tag{5.29}$$

Note that our three functions have no normal flux on faces 0, 2, and 4, so we will compute only the columns of the flux matrix for faces 1, 3, and 5. Since on f_1, $(\mathbf{x} - \mathbf{e}_1) \cdot \nu_1 = 0$, on f_3, $(\mathbf{x} - \mathbf{e}_2) \cdot \nu_3 = 0$, and on f_5, $(\mathbf{x} - \mathbf{e}_3) \cdot \nu_5 = 0$, we have

$$\begin{aligned} &\mathcal{F}_{135}(\boldsymbol{\psi}_9, \boldsymbol{\psi}_{10}, \boldsymbol{\psi}_{11}) \\ &= \begin{bmatrix} \nu_{1,1} & \nu_{3,2} & \nu_{5,3} \\ -\nu_{1,1} + 2x_2\nu_{1,2} + x_3\nu_{1,3} & \nu_{3,2} - 2x_1\nu_{3,1} - x_3\nu_{3,3} & -x_1\nu_{5,1} + x_2\nu_{5,2} \\ -x_2\nu_{1,2} + x_3\nu_{1,3} & -\nu_{3,2} + x_1\nu_{3,1} + 2x_3\nu_{3,3} & \nu_{5,2} - x_1\nu_{5,1} - 2x_2\nu_{5,2} \end{bmatrix}. \end{aligned} \tag{5.30}$$

We must add supplements that have no normal flux on faces 0, 2, and 4, and that independently span the spaces of linear polynomials on the remaining three faces.

Over $\tilde{E}$, we have that $\nu_{1,1}$, $\nu_{3,2}$, and $\nu_{5,3}$ are strictly positive. Therefore, one clear choice of 6 supplements is to take the fluxes

$$\mathcal{F}_{135}(\boldsymbol{\sigma}_0, \boldsymbol{\sigma}_1, \boldsymbol{\sigma}_2, \boldsymbol{\sigma}_3, \boldsymbol{\sigma}_4, \boldsymbol{\sigma}_5) = \begin{bmatrix} x_2 - c_2^1 & 0 & 0 \\ x_3 - c_3^1 & 0 & 0 \\ 0 & x_1 - c_1^3 & 0 \\ 0 & x_3 - c_3^3 & 0 \\ 0 & 0 & x_1 - c_1^5 \\ 0 & 1/|f_3| & -1/|f_5| \end{bmatrix}, \tag{5.31}$$

where the constants c_ℓ^i are the average over the face i of the variable x_ℓ. We conjecture that we can replace the last row by $[0 \;\; 0 \;\; x_2 - c_2^5]$, but we have not found a proof that this choice provides independent flux DOFs. Proving the conjecture reduces to showing that

$$\begin{bmatrix} c_1^1\nu_{1,1} & c_1^3\nu_{3,1} & c_1^5\nu_{5,1} \\ c_2^1\nu_{1,2} & c_2^3\nu_{3,2} & c_2^5\nu_{5,2} \\ c_3^1\nu_{1,3} & c_3^3\nu_{3,3} & c_3^5\nu_{5,3} \end{bmatrix} \tag{5.32}$$

is an invertible matrix. This matrix is simply a multiple of the identity for the cube.

A general method for handling $r = 1$ is contained in the next subsection.

5.3. The general case $r \geq 1$. In general, the DOFs of our mixed finite element spaces are allocated as

$$\begin{aligned} \mathbf{V}_r(E) &= \mathbb{P}_r^3 \oplus \mathbf{x}\tilde{\mathbb{P}}_r \oplus \mathbb{S}_r = \mathbb{E}_r \oplus \mathbb{D}_r \oplus \mathbb{B}_r \\ \text{or} \quad \mathbf{V}_r^{\text{red}}(E) &= \mathbb{P}_r^3 \oplus \mathbb{S}_r \qquad\quad\; = \mathbb{E}_r \oplus \mathbb{D}_r^{\text{red}} \oplus \mathbb{B}_r. \end{aligned} \tag{5.33}$$

Here $\mathbb{E}_r$ are the functions that have constant divergence and independently cover the normal flux DOFs (1.8). The functions in $\mathbb{D}_r$ or $\mathbb{D}_r^{\text{red}}$ match the (nonconstant) divergence DOFs (1.7). One of these functions can be constructed from a basis function in $\mathbf{x}\tilde{\mathbb{P}}_r^*$ or $\mathbf{x}\tilde{\mathbb{P}}_{r-1}^*$, respectively, but then modified by the functions in $\mathbb{E}_r$ to remove the face normal fluxes. Finally, the divergence-free bubbles $\mathbb{B}_r$ are left over, and provide the final set of DOFs. Since $\mathbb{P}_r^3 = \operatorname{curl}\mathbb{P}_{r+1}^3 \oplus \mathbf{x}\mathbb{P}_{r-1}$, we conclude that

$$\mathbb{E}_r \oplus \mathbb{B}_r = \operatorname{curl}\mathbb{P}_{r+1}^3 \oplus \mathbf{x}\mathbb{P}_0 \oplus \mathbb{S}_r. \tag{5.34}$$

Thus, our task is to construct the supplemental space $\mathbb{S}_r$ of functions with zero divergence so that the normal flux DOFs (1.8) in $\operatorname{curl}\mathbb{P}_{r+1}^3 \oplus \mathbf{x}\mathbb{P}_0 \oplus \mathbb{S}_r$ are independent.

Cockburn and Fu [11] determined the minimal number of supplemental functions (which they call "filling functions") needed to produce the space $\mathbb{E}_r$ on various elements, including a cuboidal hexahedron. In particular, [11, Lemma 4.6 and Theorems 2.10–2.15] identify the fluxes required (but note that they label the faces counting from 1 rather than 0). Their construction is to obtain supplements that have no flux on faces 0, 1, and 2. They specify the needed fluxes on face 3, but allow any flux on the last two faces. They then specify the needed fluxes on face 4, but again allow any flux on the last face. Finally, face 5 has a set of required fluxes, and these can be matched by divergence-free functions. As mentioned previously, Cockburn and Fu use a mesh of tetrahedral elements within the hexahedron to construct their supplemental functions. We can instead use the ideas of Sections 3–4.

The number of additional fluxes (see [11, Cor. 4.5 and Table 4]) is bounded by $3(r+1)$ and depends on the geometry, in particular, on the number of parallel faces. The cube requires $3(r+1)$ supplemental functions. It is numerically delicate to vary the number of supplemental functions based on the number of parallel sides, since an element E may have almost, but not quite, parallel faces.

A numerically safe way to proceed is to use the general construction of Subsection 5.1.2. Since it is difficult to characterize what functions lie in $\mathbb{B}_r$ (see, however, [11]), we simply compute the flux matrix of the entire polynomial part of the space, i.e., of a basis for $\operatorname{curl}\mathbb{P}_{r+1}^3 \oplus \mathbf{x}\mathbb{P}_0$, which has dimension $n = \dim\mathbb{P}_r^3 - \dim(\mathbf{x}\mathbb{P}_{r-1}^*) = \frac{1}{6}(r+2)(r+1)(2r+9)+1$. To proceed, it is convenient to express the flux matrix as an ordinary matrix of numbers, so we expand every normal flux polynomial in a basis that includes 1 and everything orthogonal to 1. A simple choice is displayed in (4.1) for face 1, i.e., take 1 and the functions $x_{i_1}^\ell x_{j_1}^m - c_{\ell,m}^1$ for $1 \le \ell + m \le r$. The expansion coefficients give the matrix M^{full}, which is $n \times 3(r+2)(r+1)$.

We reduce the number of rows in M^{full} to M by including only a basis for the row space. This removes the interior bubble parts of the space. It may be better to compute the singular values of M^{full} and remove all rows corresponding to small singular values. In fact, we suggest reducing M^{full} to an $n - 3(r+1)$ matrix, so that $3(r+1)$ supplements are needed, regardless of the geometry. This may create more interior bubble functions than is necessary, but it safely handles any geometry.

We proceed to find a basis N^T of $(M^T)^\perp$. Let the area vector $\boldsymbol{\varphi}$ be analogous to the one defined in (5.17) (it is the same, except that it has more zeros). The desired supplemental fluxes S are then defined by the formula in (5.18), i.e., $S = N\Big(I - \dfrac{\boldsymbol{\varphi}\boldsymbol{\varphi}^T}{\boldsymbol{\varphi}^T\boldsymbol{\varphi}}\Big)$. We construct supplemental functions $\mathbb{S}_r$ having these fluxes. By Lemma 5.1, these fluxes are independent of the ones from M, and so the space $\mathbb{E}_r$ is well-defined. Any extra functions are divergence-free bubbles, which can be modified to have no face fluxes.

We conjecture that one can chose the supplemental functions to have the highest order monomial fluxes (up to a constant) on each of the three faces 1, 2, and 3. This choice seems to work well when $r = 1$, as shown in the next section. However, we have no proof that this choice will work for any convex, cuboidal hexahedron, even when $r = 1$, as noted in the previous subsection.

In the hybrid form of the mixed method [5], the Lagrange multiplier space on the face f is simply $\mathbb{P}_r(f)$, and implementation is clear up to evaluation of the integrals over the elements. If the hybrid form is not used, one needs $H(\text{div})$-conforming finite element shape functions to from a local basis. This is done by inverting the numerical counterpart of the local flux matrix, as discussed in (5.7) for $r = 0$.

5.4. Construction of the π operator. Once the spaces $\mathbb{E}_r$, $\mathbb{D}_r$ or $\mathbb{D}_r^{\text{red}}$, and $\mathbb{B}_r$ have been determined, one can define the Raviart-Thomas [13] or Fortin [10] projection operator π_r onto $\mathbf{V}_r(E) = \mathbb{E}_r \oplus \mathbb{D}_r \oplus \mathbb{B}_r$ or π_r^{red} onto $\mathbf{V}_r^{\text{red}}(E) = \mathbb{E}_r \oplus \mathbb{D}_r^{\text{red}} \oplus \mathbb{B}_r$. One simply matches the DOFs (1.7)–(1.8) to fix the part in $\mathbb{E} \oplus \mathbb{D}_r$ or $\mathbb{E} \oplus \mathbb{D}_r^{\text{red}}$. To these DOFs, we add

$$(\mathbf{v}, \boldsymbol{\psi})_E \quad \forall \boldsymbol{\psi} \in \mathbb{B}_r. \tag{5.35}$$

These projection operators satisfy the commuting diagram property, namely, that

$$\nabla \cdot \pi_r \mathbf{v} = \mathcal{P}_{W_r} \nabla \cdot \mathbf{v} \quad \text{and} \quad \nabla \cdot \pi_r^{\text{red}} \mathbf{v} = \mathcal{P}_{W_{r-1}} \nabla \cdot \mathbf{v}, \tag{5.36}$$

where $\mathcal{P}_{W_s}$ is the L^2-projection onto W_s. Moreover, since our spaces contain full sets of polynomials, $\mathbf{V}_r \times W_r$ will have full $H(\text{div})$-approximation properties and $\mathbf{V}_r^{\text{red}} \times W_{r-1}$ will have reduced $H(\text{div})$-approximation properties. Moreover, we have the following result.

LEMMA 5.2. *The spaces $\mathbf{V}_r \times W_r$ and $\mathbf{V}_r^{\text{red}} \times W_{r-1}$ satisfy the inf-sup conditions*

$$\inf_{w \in W_r} \sup_{\mathbf{v} \in \mathbf{V}_r} \frac{(\nabla \cdot \mathbf{v}, w)_\Omega}{\|\mathbf{v}\|_{\mathbf{V}} \|w\|_W} \geq \gamma > 0 \quad \text{and} \quad \inf_{w \in W_{r-1}} \sup_{\mathbf{v} \in \mathbf{V}_r^{\text{red}}} \frac{(\nabla \cdot \mathbf{v}, w)_\Omega}{\|\mathbf{v}\|_{\mathbf{V}} \|w\|_W} \geq \gamma > 0. \tag{5.37}$$

Moreover, if $\mathbf{u}$ is sufficiently smooth and h is the diameter of the computational mesh, then

$$\|\mathbf{u} - \pi_r \mathbf{u}\| + \|\mathbf{u} - \pi_r^{\text{red}} \mathbf{u}\| \leq C h^{s+1} \|\mathbf{u}\|_{s+1}, \qquad 1 \leq s \leq r, \tag{5.38}$$

$$\|\nabla \cdot (\mathbf{u} - \pi_r \mathbf{u})\| \leq C h^{s+1} \|\nabla \cdot \mathbf{u}\|_{s+1}, \quad 1 \leq s \leq r, \tag{5.39}$$

$$\|\nabla \cdot (\mathbf{u} - \pi_r^{\text{red}} \mathbf{u})\| \leq C h^{s+1} \|\nabla \cdot \mathbf{u}\|_{s+1}, \quad 1 \leq s \leq r-1. \tag{5.40}$$

6. Some numerical results. In this section we present convergence studies for various low order mixed spaces. We include the new full and reduced spaces defined in Section 5, which we will designate as AT spaces to avoid confusion. The AT_0 space used is the simple one given in (5.5) (or, equivalently, (5.9)–(5.14)). The AT_1 full and reduced spaces used are constructed using the simple supplemental fluxes of (5.31), but with the more symmetric last row $[0 \;\; 0 \;\; x_2 - c_2^5]$.

The performance of the AT spaces will be compared to RT, BDDF, and ABF spaces. For the 3-D ABF space, we use the optimal space $\hat{\mathcal{P}}_r^{\text{opt}}(\hat{K})$ of Bergot and Durufle [6]. The test problem is defined on the unit cube $\Omega = [0, 1]^3$ with the coefficient

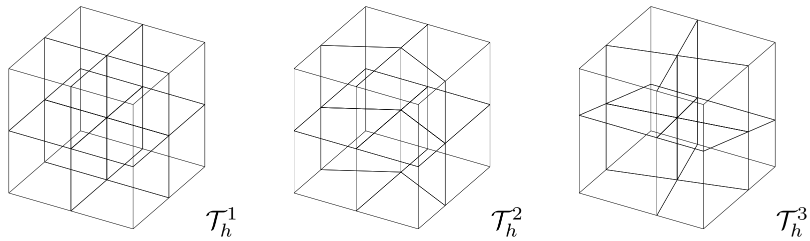

FIG. 6.1. *Mesh of $2\times2\times2$ cubes for the three base meshes. Finer meshes are constructed by repeating this base mesh pattern over the domain, appropriately reflected to maintain mesh conformity. Note that the meshes have 3, 2, and 0 pairs of parallel faces per element, respectively.*

$a = 1$ and the source function $f(\mathbf{x}) = 3\pi^2\cos(\pi x_1)\cos(\pi x_2)\cos(\pi x_3)$. The exact solution is

$$p(x_1, x_2, x_3) = \cos(\pi x_1)\cos(\pi x_2)\cos(\pi x_3), \tag{6.1}$$

$$\mathbf{u}(x_1, x_2, x_3) = \pi\begin{pmatrix}\sin(\pi x_1)\cos(\pi x_2)\cos(\pi x_3)\\ \cos(\pi x_1)\sin(\pi x_2)\cos(\pi x_3)\\ \cos(\pi x_1)\cos(\pi x_2)\sin(\pi x_3)\end{pmatrix}. \tag{6.2}$$

In the computations, we apply the hybrid form of the mixed finite element method [5]. Let $\mathcal{T}_h$ be the finite element partition of the domain Ω. For the mixed spaces $\mathbf{V}_h \times W_h$, let $\mathbf{V}_h^*$ agree with $\mathbf{V}_h$ on each element $E \in \mathcal{T}_h$, but relax the condition that the normal flux be continuous on the faces of the elements. The hybrid method is: Find $\mathbf{u}_h \in \mathbf{V}_h^*$, $p_h \in W_h$, and $\hat{p}_h \in M_h$ such that

$$(a^{-1}\mathbf{u}_h, \mathbf{v})_E - (p_h, \nabla\cdot\mathbf{v})_E + (\hat{p}_h, \mathbf{v}\cdot\nu_i)_{\partial E} = 0 \qquad \forall \mathbf{v} \in \mathbf{V}_h(E), E \in \mathcal{T}_h, \tag{6.3}$$

$$\sum_{E\in\mathcal{T}_h} (\nabla\cdot\mathbf{u}_h, w)_E = (f, w)_\Omega \qquad \forall w \in W_h, \tag{6.4}$$

$$\sum_{E\in\mathcal{T}_h} (\mathbf{u}_h\cdot\nu, \mu)_{\partial E\setminus\partial\Omega} = 0 \qquad \forall \mu \in M_h. \tag{6.5}$$

The Lagrange multiplier or trace finite element space M_h is defined locally by $M_h|_f = M_h(f) = \mathbf{V}_h\cdot\nu|_f$ for each face f of the computational mesh. For the AT spaces, $M_r(f) = \mathbb{P}_r(f)$. We require that the L^2-projection of the Dirichlet boundary condition be imposed on $\hat{p}_h$.

Solutions are computed on three different sequences of meshes. The first sequence, $\mathcal{T}_h^1$, is a uniform mesh of n^3 cubes (three sets of parallel faces per element). The second sequence, $\mathcal{T}_h^2$, is obtained from the 2-D trapezoidal meshes used in Arnold, Boffi, and Falk [4] by simply lifting them in the third direction. These elements have two pair of parallel faces per element. The third sequence of meshes, $\mathcal{T}_h^3$, is chosen so as to have no pair of faces being parallel. The first $2\times2\times2$ mesh for each sequence is shown in Fig. 6.1. Finer meshes are constructed by repeating this sub-mesh pattern over the domain, appropriately reflected to maintain mesh conformity.

The cubical mesh $\mathcal{T}_h^1$ provides a reference on which all the mixed methods work well. It turns out that the second and third meshes provide similar results, so we show only results for the most irregular case of the third mesh $\mathcal{T}_h^3$.

6.1. Full $H(\mathrm{div})$-approximation spaces. The local number of DOFs for each full $H(\mathrm{div})$-approximation finite element space can be found in Table 6.1. Note

TABLE 6.1
A comparison of the dimensions of the local RT, ABF, and AT spaces on a hexahedron E. Only the ABF and AT spaces give optimal order convergence on hexahedra.

	RT_r	ABF_r	AT_r
$\dim \mathbf{V}(E)$	$3(r+2)(r+1)^2$	$3(r+4)(r+2)^2$	$\frac{1}{2}(r+1)(r+2)(r+4)$ $+3(r+1)$ $(+2$ if $r=0)$
$\dim W(E)$	$(r+1)^3$	$(r+2)^3+3(r+2)^2$	$\frac{1}{6}(r+1)(r+2)(r+3)$
$r=0$	6 + 1	48 + 20	6 + 1
$r=1$	36 + 8	135 + 54	21 + 4

that according to Bergot and Durufle [6], the optimal ABF_0 space should satisfy the property $\mathcal{P}_E(\hat{\mathbf{V}}^0_{\mathrm{ABF}}(E)) \supset \mathbb{P}_0^3 \oplus \mathbf{x}\mathbb{P}_0$, and so it is defined to be $\hat{\mathbf{V}}^0_{\mathrm{ABF}}(E) = \mathbb{P}_{3,1,1} \times \mathbb{P}_{1,3,1} \times \mathbb{P}_{1,1,3}$. Since we solve the linear system (6.3)–(6.5) using a Schur complement for $\hat{p}_h$, we will report in this section the size of the Schur complement matrix, i.e., $\dim M_r$, rather than the size of $\dim(\mathbf{V}_r \times W_r)$.

TABLE 6.2
Errors and orders of convergence for low order RT, AT, and ABF spaces on cubical meshes.

n	n^3	M_r DOFs	$\|p-p_h\|$ error	order	$\|\mathbf{u}-\mathbf{u}_h\|$ error	order	$\|\nabla\cdot(\mathbf{u}-\mathbf{u}_h)\|$ error	order
			$\mathrm{RT}_0 = \mathrm{AT}_0$ on $\mathcal{T}_h^1$ meshes					
2	8	36	2.417e-1		1.136e-0		7.156e-0	
6	216	756	9.110e-2	0.95	4.078e-1	0.97	2.697e-0	0.95
12	1728	5616	4.609e-2	0.99	2.052e-1	0.99	1.365e-0	0.99
24	13824	43200	2.312e-2	1.00	1.027e-1	1.00	6.844e-1	1.00
			ABF_0 on $\mathcal{T}_h^1$ meshes					
2	8	144	1.035e-2		2.523e-1		2.578e-1	
6	216	3024	2.961e-4	3.17	2.786e-2	2.01	8.389e-3	3.06
12	1728	22464	3.523e-5	3.05	6.953e-3	2.00	1.031e-3	3.02
24	13824	172800	4.345e-6	3.01	1.737e-3	2.00	1.283e-4	3.00
			RT_1 on $\mathcal{T}_h^1$ meshes					
2	8	144	5.419e-2		2.440e-1		1.603e-0	
6	216	3024	6.231e-3	1.99	2.773e-2	1.99	1.845e-1	1.99
12	1728	22464	1.562e-3	2.00	6.945e-3	2.00	4.626e-2	2.00
24	13824	172800	3.909e-4	2.00	1.737e-3	2.00	1.157e-2	2.00
			AT_1 on $\mathcal{T}_h^1$ meshes					
2	8	108	1.171e-1		4.358e-1		3.465e-0	
6	216	2268	1.505e-2	1.94	5.164e-2	1.98	4.455e-1	1.94
12	1728	16848	3.814e-3	1.99	1.298e-2	1.99	1.129e-1	1.99
24	13824	129600	9.567e-4	2.00	3.249e-3	2.00	2.833e-2	2.00

In Tables 6.2–6.3, we present the errors and the orders of the convergence for the lowest two indices of the full $H(\mathrm{div})$-approximation spaces RT, AT, and ABF; although, we omit ABF_1 because the sheer size of its linear system is computationally excessive. On cubical meshes $\mathcal{T}_h^1$, RT_0 and AT_0 coincide. Table 6.2 shows first order approximation of the scalar p, the vector $\mathbf{u}$, and the divergence $\nabla\cdot\mathbf{u}$, as we should expect. The ABF_0 space gives higher order approximation of all three variables on cubes because it is constructed with higher order polynomials and, in fact, includes RT_1. The results for RT_1 and AT_1 (which are different spaces even on cubical meshes) show second order convergence for all the variables. The errors for RT_1 are smaller than AT_1, but RT_1 uses more degrees of freedom, both locally and globally.

Table 6.3 shows that for the hexahedral mesh sequence $\mathcal{T}_h^3$, RT_0 retains first order convergence of the scalar but loses convergence of the vector and divergence, while AT_0 shows first order convergence for all three quantities. The ABF_0 space still gives a higher order convergence rate for the scalar on the meshes tested. However, we can observe that the vector and divergence approximations quickly decrease to first order. We also observe that AT_1 gives the optimal second order approximation of all quantities, whereas RT_1 only retains second order for the scalar. The vector reduces to first order in this numerical test, but the results on the definition of ABF_0 [6] show that this first order convergence cannot be ensured on general meshes. The divergence appears to be converging at less than first order.

Table 6.3
Errors and orders of convergence for low order RT, AT, and ABF spaces on $\mathcal{T}_h^3$ meshes.

n	n^3	M_r DOFs	$\|p - p_h\|$ error	order	$\|\mathbf{u} - \mathbf{u}_h\|$ error	order	$\|\nabla\cdot(\mathbf{u} - \mathbf{u}_h)\|$ error	order
RT_0 on $\mathcal{T}_h^3$ meshes								
2	8	36	2.660e-1		1.185e-0		7.488e-0	
6	216	756	9.464e-2	0.94	4.591e-1	0.86	3.149e-0	0.76
12	1728	5616	4.782e-2	0.99	2.630e-1	0.75	1.952e-0	0.60
24	13824	43200	2.400e-2	1.00	1.838e-1	0.45	1.530e-0	0.29
AT_0 on $\mathcal{T}_h^3$ meshes								
2	8	36	2.661e-1		1.226e-0		7.873e-0	
6	216	756	9.452e-2	0.94	4.275e-1	0.96	2.798e-0	0.94
12	1728	5616	4.771e-2	0.99	2.150e-1	0.99	1.413e-0	0.99
24	13824	43200	2.394e-2	1.00	1.077e-1	1.00	7.087e-1	1.00
ABF_0 on $\mathcal{T}_h^3$ meshes								
2	8	144	1.474e-2		2.815e-1		3.649e-1	
6	216	3024	4.706e-4	3.04	3.697e-2	1.85	2.222e-2	2.33
12	1728	22464	6.438e-5	2.85	1.310e-2	1.47	5.909e-3	1.77
24	13824	172800	9.937e-6	2.65	5.537e-3	1.19	2.261e-3	1.30
RT_1 on $\mathcal{T}_h^3$ meshes								
2	8	144	5.644e-2		2.754e-1		1.996e-0	
6	216	3024	7.098e-3	2.03	3.688e-2	1.83	2.834e-1	1.69
12	1728	22464	1.814e-3	2.00	1.311e-2	1.47	1.239e-1	1.15
24	13824	172800	4.541e-4	2.00	5.547e-3	1.19	7.382e-2	0.64
AT_1 on $\mathcal{T}_h^3$ meshes								
2	8	108	1.299e-1		4.526e-1		3.846e-0	
6	216	2268	1.600e-2	1.95	5.629e-2	2.00	4.737e-1	1.95
12	1728	16848	4.091e-3	1.98	1.436e-2	1.99	1.211e-1	1.98
24	13824	129600	1.027e-3	2.00	3.600e-3	2.00	3.040e-2	2.00

6.2. Reduced $H(\mathrm{div})$-approximation spaces. Next we consider the reduced H(div)-approximation spaces BDDF_1 and $\mathrm{AT}_1^{\mathrm{red}}$, which coincide on cubical meshes. These spaces have the same local and global dimension, as shown in Table 6.4. The

Table 6.4
The dimensions of the local BDDF and $AT^{\rm red}$ spaces on a hexahedron E. These spaces coincide on rectangles, and they have the same local dimension. Only the $AT^{\rm red}$ spaces give optimal order convergence on hexahedra.

	BDDF, $\mathrm{AT}_r^{\rm red}$
$\dim\mathbf{V}(E)$	$\frac{1}{2}(r+1)(r+2)(r+3)+3(r+1)$
$\dim W(E)$	$\frac{1}{6}r(r+1)(r+2)$
$r=1$	18 + 1

Table 6.5
Errors and orders of convergence for $BDDF_1$ and $AT_1^{\rm red}$.

n	n^3	M_r DOF	$\|p-p_h\|$ error	order	$\|\mathbf{u}-\mathbf{u}_h\|$ error	order	$\|\nabla\cdot(\mathbf{u}-\mathbf{u}_h)\|$ error	order
$\mathrm{BDDF}_1 = \mathrm{AT}_1^{\rm red}$ on $\mathcal{T}_h^1$ meshes								
2	8	108	2.417e-1		5.611e-1		7.156e-0	
6	216	2268	9.114e-2	0.95	8.601e-2	1.85	2.697e-0	0.95
12	1728	16848	4.610e-2	0.99	2.249e-2	1.95	1.365e-0	0.99
24	13824	129600	2.312e-2	1.00	5.701e-3	1.98	6.844e-1	1.00

computational results appear in Tables 6.5–6.6. As we expect, the elements give first order approximation for the scalar p and the divergence $\nabla\cdot\mathbf{u}$ and second order convergence for the vector $\mathbf{u}$ on cubical meshes, as shown in Table 6.5. On the hexahedral meshes $\mathcal{T}_h^3$, Table 6.6 shows that BDDF_1 has first order approximation of the scalar but loses convergence of the vector and the divergence. When $\mathrm{AT}_1^{\rm red}$ is used instead, the optimal convergence rates of the cubical meshes are recovered for the hexahedral meshes, i.e., second order approximation for the vector $\mathbf{u}$ and first order for the scalar p and the divergence $\nabla\cdot\mathbf{u}$.

Table 6.6
Errors and orders of convergence for $BDDF_1$ and $AT_1^{\rm red}$.

n	n^3	M_r DOF	$\|p-p_h\|$ error	order	$\|\mathbf{u}-\mathbf{u}_h\|$ error	order	$\|\nabla\cdot(\mathbf{u}-\mathbf{u}_h)\|$ error	order
BDDF_1 on $\mathcal{T}_h^3$ meshes								
2	8	108	2.665e-1		6.450e-1		7.487e-0	
6	216	2268	9.481e-2	0.94	1.164e-1	1.52	3.149e-0	0.76
12	1728	16848	4.786e-2	0.99	4.000e-2	1.43	1.952e-0	0.60
24	13824	129600	2.401e-2	1.00	1.723e-2	1.16	1.530e-0	0.29
$\mathrm{AT}_1^{\rm red}$ on $\mathcal{T}_h^3$ meshes								
2	8	108	2.660e-1		6.435e-1		7.876e-0	
6	216	2268	9.455e-2	0.94	9.760e-2	1.76	2.798e-0	0.94
12	1728	16848	4.772e-2	0.99	2.610e-2	1.91	1.413e-0	0.99
24	13824	129600	2.394e-2	1.00	6.753e-3	1.96	7.087e-1	1.00

REFERENCES

[1] T. Arbogast and M. R. Correa, *Two families of H(div) mixed finite elements on quadrilaterals of minimal dimension*, SIAM J. Numer. Anal., 54 (2016), pp. 3332–3356. DOI 10.1137/15M1013705.

[2] D. N. Arnold and G. Awanou, *Finite element differential forms on cubical meshes*, Math. Comp., 83 (2014), pp. 1551–1570.

[3] D. N. Arnold, D. Boffi, and F. Bonizzoni, *Finite element differential forms on curvilinear cubic meshes and their approximation properties*, Numer. Math., 129 (2015), pp. 1–20.

[4] D. N. Arnold, D. Boffi, and R. S. Falk, *Quadrilateral H(div) finite elements*, SIAM. J. Numer. Anal., 42 (2005), pp. 2429–2451.

[5] D. N. Arnold and F. Brezzi, *Mixed and nonconforming finite element methods: Implementation, postprocessing and error estimates*, RAIRO Modél. Math. Anal. Numér., 19 (1985), pp. 7–32.

[6] M. Bergot and M. Duruflé, *Approximation of H(div) with high-order optimal finite elements for pyramids, prisms and hexahedra*, Communications in Computational Physics, 14 (2013), pp. 1372–1414.

[7] F. Brezzi, J. Douglas, Jr., R. Duràn, and M. Fortin, *Mixed finite elements for second order elliptic problems in three variables*, Numer. Math., 51 (1987), pp. 237–250.

[8] F. Brezzi, J. Douglas, Jr., M. Fortin, and L. D. Marini, *Efficient rectangular mixed finite elements in two and three space variables*, RAIRO Modél. Math. Anal. Numér., 21 (1987), pp. 581–604.

[9] F. Brezzi, J. Douglas, Jr., and L. D. Marini, *Two families of mixed elements for second order elliptic problems*, Numer. Math., 47 (1985), pp. 217–235.

[10] F. Brezzi and M. Fortin, *Mixed and hybrid finite element methods*, Springer-Verlag, New York, 1991.

[11] B. Cockburn and G. Fu, *Superconvergence by M-decompositions. Part III: Construction of three-dimensional finite elements*, ESAIM: Mathematical Modelling and Numerical Analysis, 51 (2017), pp. 365–398.

[12] R. S. Falk, P. Gatto, and P. Monk, *Hexahedral H(div) and H(curl) finite elements*, ESAIM Math. Model. Numer. Anal., 45 (2011), pp. 115–143.

[13] R. A. Raviart and J. M. Thomas, *A mixed finite element method for 2nd order elliptic problems*, in Mathematical Aspects of Finite Element Methods, I. Galligani and E. Magenes, eds., no. 606 in Lecture Notes in Math., Springer-Verlag, New York, 1977, pp. 292–315.

[14] J. Shen, *Mixed finite element methods on distorted rectangular grids*, Tech. Rep. ISC-94-13-MATH, Institute for Scientific Computation, Texas A&M University, College Station, Texas, 1994.

[15] J. M. Thomas, *Sur l'analyse numerique des methodes d'elements finis hybrides et mixtes*, PhD thesis, Sciences Mathematiques, à l'Universite Pierre et Marie Curie, 1977.